Original paper

A comparative assessment of inhomogeneity and finite patient dimension effects in ^{60}Co and ^{192}Ir high-dose-rate brachytherapy

Irina Fotina, PhD[1], Kyveli Zourari, PhD[2], Vasileios Lahanas, PhD[2], Evaggelos Pantelis, PhD[2], Panagiotis Papagiannis, PhD[2]

[1]Eckert & Ziegler BEBIG GmbH, Berlin, Germany, currently at: Department of Radiation Oncology, King Hamad University Hospital, Kingdom of Bahrein, [2]Medical Physics Laboratory, Medical School, National and Kapodistrian University of Athens, Greece

Abstract

Purpose: To perform a comparative study of heterogeneities and finite patient dimension effects in ^{60}Co and ^{192}Ir high-dose-rate (HDR) brachytherapy.

Material and methods: Clinically equivalent plans were prepared for 19 cases (8 breast, 5 esophagus, 6 gynecologic) using the Ir2.A85-2 and the Co0.A86 HDR sources, with a TG-43 based treatment planning system (TPS). Phase space files were obtained for the two source designs using MCNP6, and validated through comparison to a single source dosimetry results in the literature. Dose to water, taking into account the patient specific anatomy and materials ($D_{w,m}$), was calculated for all plans using MCNP6, with input files prepared using the BrachyGuide software tool to analyze information from DICOM RT plan exports.

Results: A general TG-43 dose overestimation was observed, except for the lungs, with a greater magnitude for ^{192}Ir. The distribution of percentage differences between TG-43 and Monte Carlo (MC) in dose volume histogram (DVH) indices for the planning target volume (PTV) presented small median values (about 2%) for both ^{60}Co and ^{192}Ir, with a greater dispersion for ^{192}Ir. Regarding the organs at risk (OARs), median percentage differences for breast $V_{50\%}$ were 3% (5%) for ^{60}Co (^{192}Ir). Differences in median skin D_{2cc} were found comparable, with a larger dispersion for ^{192}Ir, and the same applied to the lung D_{10cc} and the aorta D_{2cc}. TG-43 overestimates D_{2cc} for the rectum and the sigmoid, with median differences from MC within 2% and a greater dispersion for ^{192}Ir. For the bladder, the median of the difference is greater for ^{60}Co (~2%) than for ^{192}Ir (~0.75%), demonstrating however a greater dispersion again for ^{192}Ir.

Conclusions: The magnitude of differences observed between TG-43 based and MC dosimetry and their smaller dispersion relative to ^{192}Ir, suggest that ^{60}Co HDR sources are more amenable to the TG-43 assumptions in clinical treatment planning dosimetry.

J Contemp Brachytherapy 2018; 10, 1: 73-84
DOI: https://doi.org/10.5114/jcb.2018.74327

Key words: ^{60}Co, ^{192}Ir, HDR, TG-43, treatment planning.

Purpose

The availability of miniaturized ^{60}Co sources introduced an alternative to ^{192}Ir sources in high-dose-rate (HDR) brachytherapy applications, with an advantage in terms of resource and workload sparing. The latter stems from the difference in source exchange frequency, owing mainly to the difference in the half-life of the two radionuclides.

This development led to several comparative studies published in the literature. These include comparative evaluations of acute toxicity in gynecological cancer [1,2], and dosimetry studies ranging from single source dosimetry comparison [3,4,5] to comparisons of dose distributions in gynecological [4,5,6,7], prostate [8], skin [9], and breast [10,11,12] HDR brachytherapy treatments using different techniques. In a comprehensive dosimetry study, Palmer *et al*. [6] correctly pointed out that the common use of plans with identical source dwell loading patterns for ^{192}Ir and ^{60}Co is informative only with regard to the inherent physical difference between the sources used. These authors compared dosimetry of a clinical treatment planning system (TPS) for eight cervix cancer patients using ^{192}Ir and ^{60}Co sources in plans with identical dwell positions and relative times, as well as plans optimized independently for each source by a single experienced planner [6].

One aspect that has not been systematically reviewed in the literature is the relative importance of patient inhomogeneities and bounded dimensions in ^{192}Ir and ^{60}Co HDR brachytherapy. This is timely, since brachytherapy has recently advanced towards individualized planning

Address for correspondence: Panagiotis Papagiannis, PhD, Medical Physics Laboratory, Medical School, National and Kapodistrian University of Athens, Greece, Medical Physics Lab., Medical School Mikras Asias 75, Goudi, 11527 Athens, Greece, phone: +30 2107462442, ✉ e-mail: ppapagi@med.uoa.gr

Received: 24.10.2017
Accepted: 19.01.2018
Published: 28.02.2018

dosimetry with the commercial availability of TPSs, including image-based dose calculation algorithms as an option for ^{192}Ir HDR treatments [13,14]. Image-based dose calculation algorithms mark an improvement over TG-43 based planning dosimetry. While TG-43 based algorithms rely on source specific data pre-calculated in a standard sized geometry of homogeneous water [15], therefore disregarding patient-specific radiation scatter conditions and the radiological differences of tissue or applicator materials from water, the new algorithm options exploit information derived from patient imaging to account for these effects [13].

While the influence of patient specific scatter and inhomogeneities is intuitively expected to be less with increasing photon energy, a systematic study is required for a comparative assessment of the effect in clinical terms. Such a study is not insignificant since:

- the effects vary with treatment site and, possibly, patient geometry, so appropriate patient samples are required;
- dual plans must be generated for each patient with a clinical TPS using ^{192}Ir and ^{60}Co sources. These plans must be independently optimized, to reflect best clinical practice with each source, and clinically equivalent, so that no bias is introduced in the comparison of the studied effects between ^{192}Ir and ^{60}Co;
- dosimetry must be repeated for each plan using a reference method capable of accurately accounting for the studied effects for both sources, such as Monte Carlo (MC) simulation;
- MC simulation must be benchmarked against TG-43 single source dosimetry to ensure there is no bias in the assessment of the studied effects for each source, which would affect the comparison between ^{192}Ir and ^{60}Co.

In this work, data from a group of patients treated with HDR brachytherapy for breast, esophagus, and cervical cancer are used. Treatment planning was performed with an ^{192}Ir and a ^{60}Co HDR source, using the same commercially available, TG-43 based, TPS, and the same plan acceptance criteria. MC simulation was performed for each of the generated plans, and results were compared to corresponding TG-43 based planning dosimetry to assess the relative importance of accounting for patient specific scatter conditions and inhomogeneities in ^{192}Ir and ^{60}Co HDR brachytherapy.

Material and methods

Treatment planning dosimetry

A group of 19 consecutive (randomly pooled) patients was formed, including 8 breast, 5 esophagus, and 6 cervical cancer cases. Dual treatment plans were created using the SagiPlan® v.2.0 TPS (Eckert & Ziegler BEBIG, Germany) with the Co0.A86 [16] and the Ir2.A85-2 [17] HDR sources. In order to mitigate any bias, the treatment plans were created de novo by a single planner, using the same plan acceptance criteria for both sources.

Breast cases correspond to a brachytherapy boost following conservative surgery and whole breast irradiation. Rigid stainless steel (SS) needles of 0.85 mm radius had been used for the implants (median, 15; range, 6-16). After activating the dwell positions within the planning target volume (PTV) with a 2-3 mm margin, geometrical optimization was performed and 10 Gy were prescribed to the surface of the target. Manual adaptation of the isodoses was then performed to achieve similar target coverage (V_{90} > 90%, dose homogeneity index, DHI > 0.7), and minimize V_{200}. The median number of dwell positions used was 83 for ^{60}Co (range, 55-113) and 78 for ^{192}Ir (range, 36-148). A constant transmission factor was applied by the SagiPlan TPS to TG-43 based dose calculation results (equal to 0.995 and 0.992 for ^{60}Co and ^{192}Ir, respectively) to account for the attenuation of radiation emitted from a source in a SS applicator. This approach does not account for the interposition of multiple SS applicators between a source dwell position and a dose calculation point.

For the esophagus treatments, a dose prescription of 5 Gy to a reference group of points at 1 cm distance from the plastic applicator central axis was applied using graphical adjustment of isodose lines, as required to ensure CTV coverage (D_{90} > 95%). The median number of dwell positions in the single plastic catheter inserted into the esophagus was 10 for ^{60}Co (range, 5-15) and 8 for ^{192}Ir (range, 5-14).

The cervical cases comprised three treatments using the interstitial CT/MR ring applicator set-60º (set 0152 [18]), two using the SS intrauterine tube set (set 0108 [18]), and one with a custom applicator (plastic cylinder bearing holes for plastic interstitial catheters and an external template for extra plastic catheters). A standard source loading was used for creating single fraction plans with a prescription of 5-7 Gy to point A [19], and manual isodose optimization to adjust bladder and rectum D_{2cc} values. The number of source dwell positions used were 15, 20, and 13 for both ^{60}Co and ^{192}Ir plans for the cases employing the ring applicator, 7 SS applicators in the first sequential case were loaded with 87 and 76 source dwell positions, 1 SS applicator in the second sequential case with 16 and 15 source dwell positions, and 13 plastic needles with the custom applicator loaded with 79 and 65 source dwell positions, for the ^{60}Co and ^{192}Ir plans, respectively. While the treatment planning methods employed may differ from local protocols or contemporary codes of practice, the dose distributions produced are characteristic of the cases studied, and thus fulfill the scope of this study.

The structures considered for the purpose of this work included the PTV and organs at risk (OARs) as appropriate for each treatment site (lung, rib, and skin for the breast cases; lung, aorta, and trachea for the esophageal cases; rectum, sigmoid, and bladder for the gynecological cases). For the breast cases, the ribs adjacent to the PTV were contoured for every patient. The skin was defined using a 5 mm (skin-5mm) contraction of the external patient contour. The 5 mm thickness was used to account for dose to the skin vasculature that correlates to skin toxicity [20].

The treatment plans generated were exported from the TPS in DICOM RT format.

Monte Carlo dosimetry

The MCNP v.6.1 Monte Carlo (MC) code [21] was employed for all MC simulations of this work, using the EPDL97 cross section data library (https://www-nds.iaea.org/epdl97/) [22].

Single source simulations

Efficiency improvement was considered as essential in this work, in view of the large number of simulations required (2 multi catheter/source dwell position plans, for each of the 19 patients studied). Besides automating the preparation of simulation input files from patient dicom RT plans, the BrachyGuide software tool [23] employed (see next section) improves MC simulation efficiency through representing sources in the generated input files by means of pre-calculated, source-specific phase space files. Single source MC simulations were therefore performed to calculate the required phase space files.

Source models for the Co0.A86 and the Ir2.A85-2 were configured using information provided by the manufacturer. Photons were generated uniformly inside the active core of each source according to emission spectra taken from the National Nuclear Data Center [24]. Electron emissions were not considered in these simulations. Tracking was performed only for photons. Bremsstrahlung production was not modeled in view of the low radiation yield for electron energies under 1.5 MeV in the source materials. The scoring region defined for storing, the phase space data of photons emitted from the outer surface of the sources consisted of a cylindrical surface encompassing the sources (0.1 cm and 0.09 cm diameter for the Co0.A86 and the Ir2.A85-2, respectively), and two planes at the source tips and cable drive wires. The same number of photon histories was simulated for both sources (10^8). The energy, position, direction, and weight of the photons exiting the phase space scoring region (~10^8 and 9 x 10^7 photons for the Co0.A86 and the Ir2.A85-2, respectively) were stored in a corresponding file of 9.6 GB and 8.2 GB in binary format [25]. Simulations for phase space file calculations were performed with the sources centered in a water phantom, so as to score the dose distribution in TG-43 conditions in the same run. The water phantom dimensions (100 cm and 40 cm radius for the Co0.A86 and the Ir2.A85-2, respectively) were chosen, so that full scatter conditions were fulfilled at points of dosimetric interest and in accordance with studies on the TG-43 dosimetric characterization of the sources in the literature [16,17]. Water collisional kerma K was scored using the *FMESH4 tally in a cylindrical mesh, defined for distances up to 15 cm along the source transverse bisector and each direction of the source longitudinal axis, with a 0.1 cm resolution in thickness and height. This tally scores the energy fluency, averaged over each mesh cell in units of MeV cm^{-2} per starting photon, which was converted to MeV g^{-1} per starting photon using the mass energy absorption coefficients of water taken from NIST [26], along with a dose energy and dose function (DE/DF) card [21]. The statistical uncertainty of results was less than 1% for the majority of points in the simulated geometry, increasing to 2% at points close to the source longitudinal axis, and 3% only at a few points close to the source longitudinal axis at relatively increased radial distance, for both sources.

The phase space files obtained as described above do not include electron emissions from ^{192}Ir and ^{60}Co. Therefore, their use in patient specific MC simulations inherently assumes that dose from electron emissions D_e is negligible relative to dose from photon emissions D_γ. This is a safe assumption for the sources considered in this work [16,17], which enhances simulation efficiency. Additional efficiency improvement in patient specific MC simulations of this work can be achieved by not simulating secondary electron transport, i.e., assume that electronic equilibrium applies to all points around the sources, and D_γ can therefore be approximated by collisional kerma K. This assumption, however, warrants further investigation for the relatively higher energies of ^{60}Co [27,28]. Two additional single source MC simulations were hence performed for the Co0.A86 HDR source to estimate the effect of electronic disequilibrium close to material interfaces.

In the first run, the Co0.A86 source was centered in a 50 cm radius water sphere. D_γ was scored with 0.1 mm resolution, using cylindrical cells at distances from the source center $r \leq 10$ mm, using the *F8:p,e tally. This tally scores energy distribution of pulses created in a detector in units of MeV, which was converted to MeV g^{-1} per starting photon using the mass density of each scoring cell. K was scored at the same cells using the *F4:p tally converted to MeV g^{-1} per starting photon, as described above for the *FMESH4 tally. The number of initial photon histories simulated was 10^9, and the type A uncertainty of MC results using the estimated relative error at the 1σ level, as this was calculated by the MC code, was 0.7% and 0.2% for D_γ and K, respectively. An additional benchmarking run was performed for the same spherical ^{60}Co source employed by Ballester *et al*. [28] to mimic the BEBIG source model [16]. This comprised a pure cobalt core with a 0.15 mm stainless steel encapsulation and an outer diameter of 0.5 mm. D_γ and K were scored with a 0.1 mm resolution, using cylindrical cells at distances $r \leq 10$ mm from the source center, using the *F8:p,e tally and the *F4:p tallies as described above.

In the second run, two cubes of 2 cm edge were added to the simulated geometry. These were centered at ±4 cm on either side of the source, along its transverse bisector. One consisted of cortical bone and the other of inflated lung tissue [29]. D_γ was scored with a 0.1 cm resolution, using cubical cells of 0.1 × 0.1 × 0.1 cm^3 lying along the source transverse bisector, for distances from the source center $r \leq 5$ cm, using the *F8:p,e tally. Water K was also estimated at the same scoring grid, using the *FMESH4:p superimposed mesh tally. The number of initial photon histories simulated was 10^9 and the type A uncertainty of MC results, according to the relative error at the 1σ level estimated by the MC code, were 2% and 0.8%, for D_γ and K, respectively.

Patient-specific simulations

Input files for patient specific MC simulations were automatically created from corresponding CT images and

DICOM-RT treatment plan data, using the BrachyGuide software tool [23], which is distributed freely over the internet (www.rdl.gr/downloads). BrachyGuide has been amended to parse dicom RT information from plans exported from the SagiPlan TPS, using the corresponding dicom conformance statement. The configuration of input files for MC simulation using BrachyGuide has been described in detail in the literature [23,30,31,32]. In brief, computational models were represented through rectangular lattice geometry. The size of each lattice element was equal to the voxel size of the imported patient CT images. Mass density was determined on a voxel-by-voxel basis, using a default CT calibration of Hounsfield units (HU) versus density. Mass density is used to assign elemental composition to each voxel using a look-up table of 23 human tissue composition bins [29,33], which was augmented by two materials (titanium and stainless steel) to account for the applicators in the gynecological cancer cases studied. Further processing was required only for the studied breast cases, due to streaking artefacts from the rigid SS needles. These were locally corrected by assigning material as female soft tissue. In order to account for the attenuation effects of the SS applicators in the MC simulations, these were created independently and superimposed on the lattice geometry of the input file. The source was represented by a pre-calculated, source-specific phase space file in the generated input files (see previous section). A transformation was applied to each photon position and direction read from the phase space file to account for source dwell position and the source orientation. This matrix is calculated by BrachyGuide for each dwell position in a treatment plan, based on information retrieved from the corresponding RT plan and RT structure set data. The matrix to be applied is sampled from a probability distribution, calculated using the fraction of source dwell times by total irradiation time. Absorbed dose was approximated by water collision kerma, and the *FMESH4 tally superimposed over the simulated model geometry was used to score water kerma in medium, $K_{w,m}$, in voxels of size equal to that of the lattice geometry elements for each patient, over the spatial extent of the RT dose data. Results were converted to MeV g^{-1} per starting photon, using water mass energy absorption coefficients taken from NIST [26], along with a dose energy and function (DE/DF) card [21]. A tally multiplier proportional to the ratio of total reference air kerma (TRAK) of the corresponding treatment plan by the nominal air kerma strength of the source, determined in a separate MC run, was added to the MC input file to convert MC output data from $MeVg^{-1}$ per starting particle to Gy. The same number of photon histories was simulated for all patients, equal with the number of photons recorded on the phase space file of each source (~10^8 and ~8 x 10^7 for ^{60}Co and ^{192}Ir, respectively). The type A uncertainty of the simulations was evaluated using the relative error at the 1σ level estimated by the MC code. This was typically less than 1% at distances less than 5 cm from the implant for both ^{60}Co and ^{192}Ir, and reached 1.9% (2.3%) at the edges of the calculation grid for ^{60}Co (^{192}Ir).

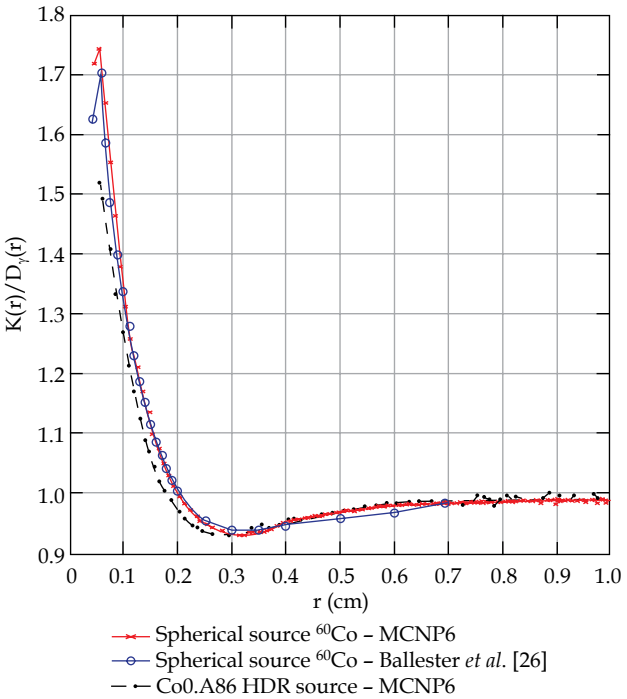

Fig. 1. Ratio of collisional kerma K to photon dose Dγ as a function of radial distance for a spherical ^{60}Co source resembling commercially available sources, and the Co0.A86 high-dose-rate (HDR) ^{60}Co source. Corresponding Monte Carlo (MC) simulation results of Ballester *et al.* [26] for the same spherical source are also presented for comparison

Treatment plan evaluation and dosimetry comparison

TG-43 data in DICOM RT dose format and corresponding MC output for each patient were imported into the BrachyGuide software. The former was interpolated to the resolution of the latter (the CT resolution of the imaging set for each patient), and comparison was performed in terms of the spatial distribution of percentage dose differences of TG-43 from corresponding MC results. Results were also compared in terms of the relative cumulative dose volume histograms (DVHs) for the PTV and the OARs, which were calculated in BrachyGuide using 1% relative dose intervals. The comparison included indices for the volume or percentage of a structure receiving dose greater than given values or prescribed dose percentages, and the minimum prescribed dose percentages delivered at given volumes or percentages of a structure.

Results

Single source simulations

Figure 1 presents results of simulations performed to study the effect of electronic disequilibrium close to a ^{60}Co source. Results of Ballester *et al.* [28] for a spherical ^{60}Co source of materials and dimensions resembling commercially available sources are also presented in Figure 1 for comparison to corresponding results of this work. Besides the fact that electron emissions were not simulated in this work, and K/D_γ results of this work are compared

to $K/(D_e+D_\gamma)$ results from [28], a close agreement is observed (within 1% except for the first couple of points, where agreement is within 2.3% and 6%, respectively) serving as a validation of MC methods used in this work.

The ratio of K to D_γ for the Co0.A86 HDR source is also presented in Figure 1. Comparison to corresponding results for the spherical ^{60}Co source shows close agreement for distances greater than 3 mm from the source center. This supports the conclusion that electronic equilibrium conditions obtained for spherical sources could be generalized to actual sources [34]. Most important, these results show that electronic disequilibrium affects dosimetry more than 2% at distances less than 7 mm from the source center. It was therefore decided to employ the approximation of dose by collisional kerma in patient-specific simulations of this work to promote efficiency, and disregard the high-dose volume close to the sources, when comparing TG-43 and MC results. This approximation does not affect other parts of the patient-specific geometries, since an electronic disequilibrium effect was not detected at the interface between water and lung or bone in MC results (see Supplementary Figure 1).

Single source MC simulation results of this work (corrected for electronic disequilibrium for the Co0.A86 source) were compared with corresponding consensus data [35] taken from single publications for each source [16,17] (see Supplementary Figure 2 and 3). Dose rate constants were found to agree within statistical uncertainty, and radial dose function as well as anisotropy function results were typically within 1%. Greater differences were observed only for anisotropy at points close to the drive wire of the sources. Given that the same input data and drive wire length were assumed in simulations in this work and the literature [16,17], these differences are probably due to the combined effect of subtle differences in the source designs (e.g., core and stainless steel densities, simulation of air gap within the source, etc.) and MC methods used. These differences are not expected to bias the comparison of differences between TG-43 and MC results in patient plans prepared with the Co0.A86 and the Ir2.A85-2 sources, especially since the high-dose volume close to the sources is discarded from the comparison.

Patient-specific simulations

Indicative dose distribution comparisons

Figure 2 presents TG-43 and MC dosimetry results for an indicative breast case, in the form of isodose lines superimposed on a colormap of pixel-by-pixel percentage dose differences relative to MC, for the ^{60}Co and the ^{192}Ir treatment plans, on axial, sagittal, and coronal planes. Target and OARs contours are also delineated on Figure 2. For the PTV, TG-43 and MC results are in good agreement for both treatment plans, with a TG-43 overestimation of the order of 2%, except for points close to the catheters/source dwell positions. These points are subject to the combined effects of electronic disequilibrium close to the Co0.A86 source (which is not taken into account in MC results). The application of a constant transmission factor to TG-43 based dose calculations, and mainly, the fact that voxels within or partially including, the applicators are not excluded in Figure 2. Regarding the rib and the skin of OARs in the ^{60}Co plan, a TG-43 overestimation is observed ranging from 2% to 6% at points away from the implant. For the lung, TG-43 overestimates dose by up to 4% close to the implant, and underestimates dose substantially at increased distances (up to 6%). Considerably greater differences can be observed in Figure 2 between TG-43 and MC calculations for the ^{192}Ir plan. The TG-43 overestimation is of the order of 8% close to the implant reaching up to 20% away. Inside the lung, TG-43 overestimates dose by up to 10% close to the implant, and underestimates dose substantially (up to 6%) at increased distances. For the skin, local dose differences also depend on the distance from the implant reaching up to 20%. Regarding the rib, differences between TG-43 and MC calculations are of the order of 4%-8% (relative to 2-4% for ^{60}Co).

Figure 3 presents a similar comparison between TG-43 and MC dosimetry results for an indicative esophagus case. Considerably greater differences can be observed between TG-43 and MC calculations for the ^{192}Ir plan for isodose lines lower than 20%, which are position dependent. For the right lung, TG-43 differences from MC dosimetry results are comparable for the ^{60}Co and the ^{192}Ir treatment plans. For the right lung, TG-43 overestimates dose close to the catheter (4% and 6% for the ^{60}Co and the ^{192}Ir plan, respectively), and underestimates dose at increased distances (16% and 20% for the ^{60}Co and the ^{192}Ir plan, respectively). For the left lung, differences between TG-43 and MC results follow the same pattern, being however greater in magnitude for the ^{192}Ir plan.

Figure 4 presents the same comparison between TG-43 and MC for an indicative cervical treatment. A general dose overestimation by TG-43 is observed, which appears to affect OARs dosimetry more for the ^{192}Ir plan. For the ^{60}Co plan, the overestimation is of the order of ~2%, reaching up to ~8-10% at increased distances within the 10% isodose line. For the ^{192}Ir plan, TG-43 overestimates dose by ~2%-4% at distances close to the implant, and up to 18% at points within the 50% isodose line.

Patient group DVH comparisons

The comparison of TG-43 and MC dosimetry is presented in Figures 2-4 on given planes for selected patient cases, illustrative of the pattern of differences due to the physics underlying dose delivery with the ^{60}Co and the ^{192}Ir sources. Nevertheless, a comparison in terms of DVH indices in the studied patient groups is required to count in 3D patient anatomy and a variation of these differences within each group.

This comparison is presented in Figure 5 for the breast patient group. In Figure 5A, a general TG-43 overestimation of the PTV related indices are observed for both ^{60}Co and ^{192}Ir. Median differences are comparable for coverage, presenting however a larger dispersion as well as some instances of underestimation for ^{192}Ir. DVH indices for the OARs are summarized in Figure 5B. As shown in this figure, TG-43 overestimates dose to the healthy breast tissue, with median percentage differences from MC results of the order of 3% and 5% for ^{60}Co and ^{192}Ir, respectively. Regarding the skin structures studied in this

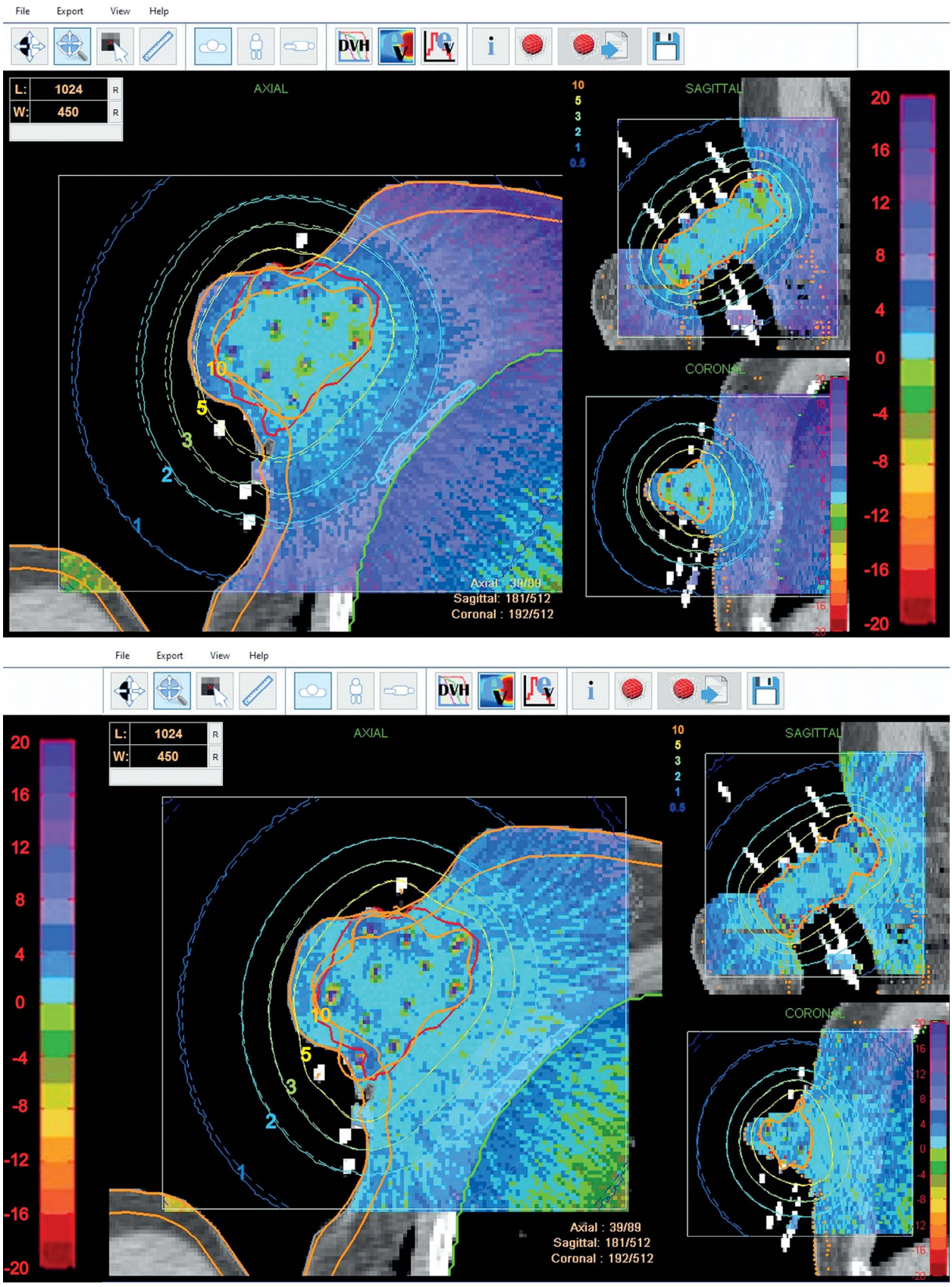

Fig. 2. Comparison of TG-43 and Monte Carlo (MC) dosimetry results for an indicative breast case, in the form of isodose lines and a colormap of pixel-by-pixel percentage dose differences ((D_(TG-43)-D_MC)/D_MC) superimposed on patient images, for the ^{60}Co (Figure 2 top) and the ^{192}Ir (Figure 2 bottom) treatment plans. Selected isodose lines (in units of Gy) are also presented

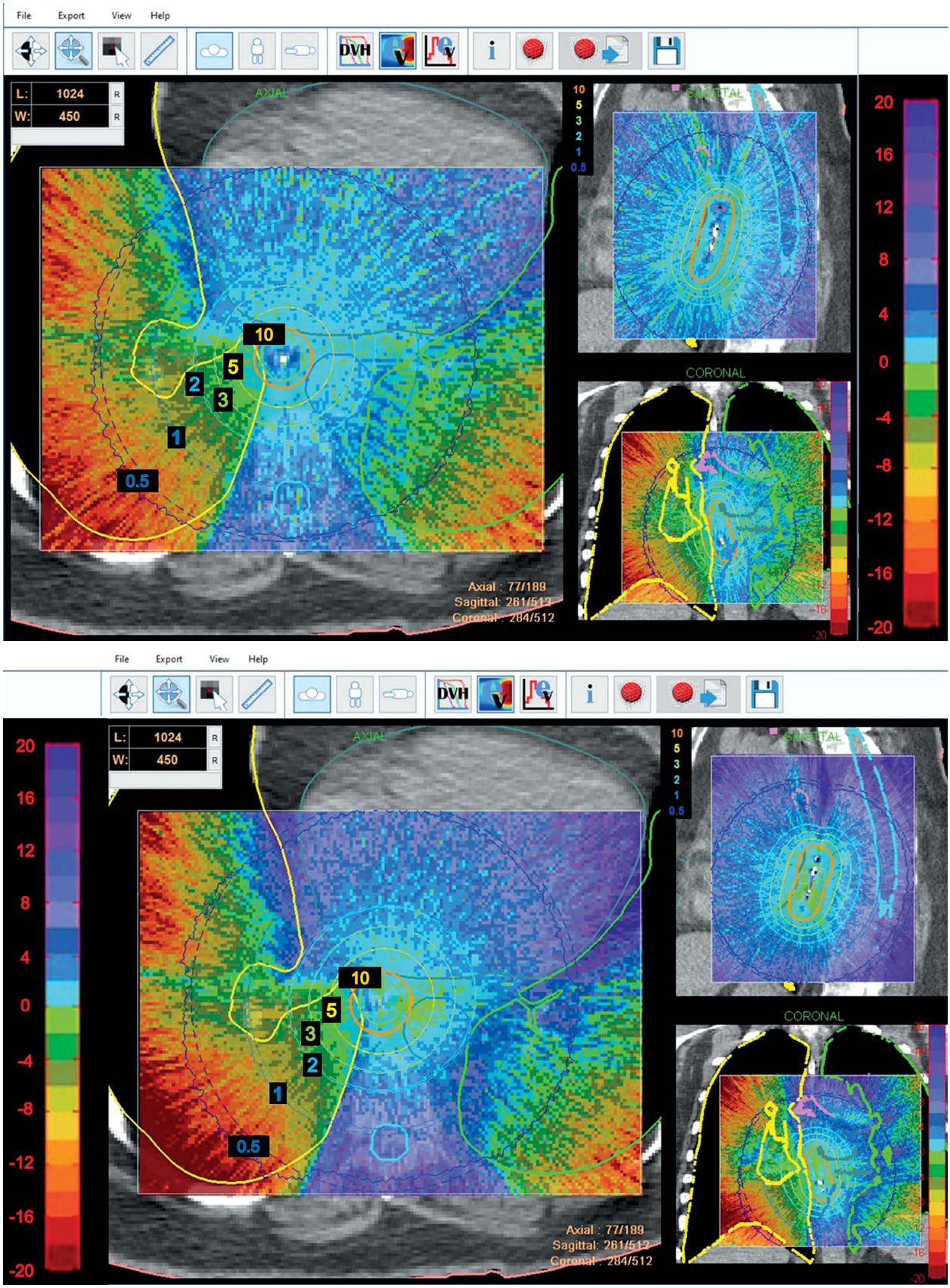

Fig. 3. Same as Figure 2, for an indicative esophagus treatment case

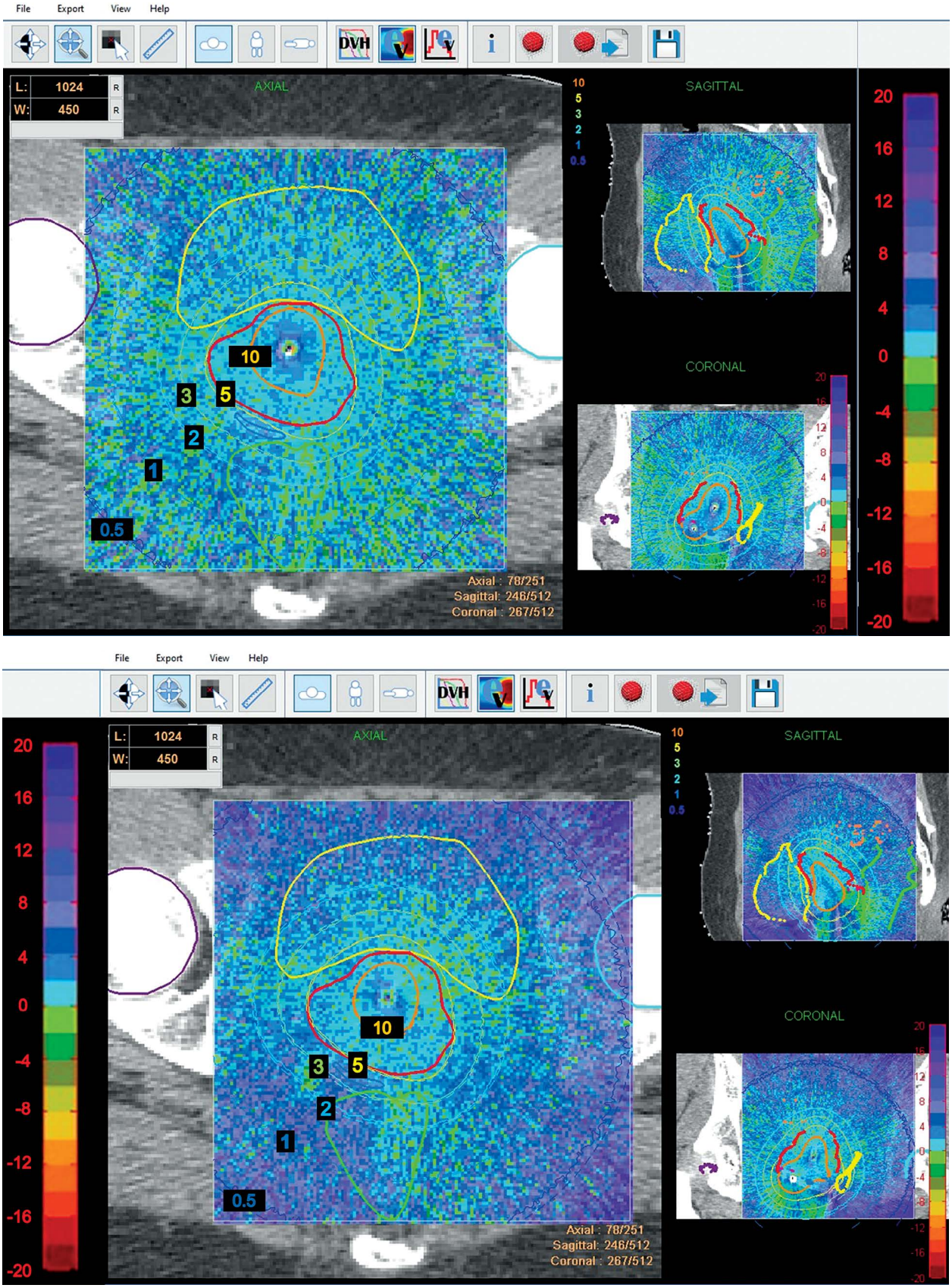

Fig. 4. Same as Figure 2, for an indicative cervical treatment case

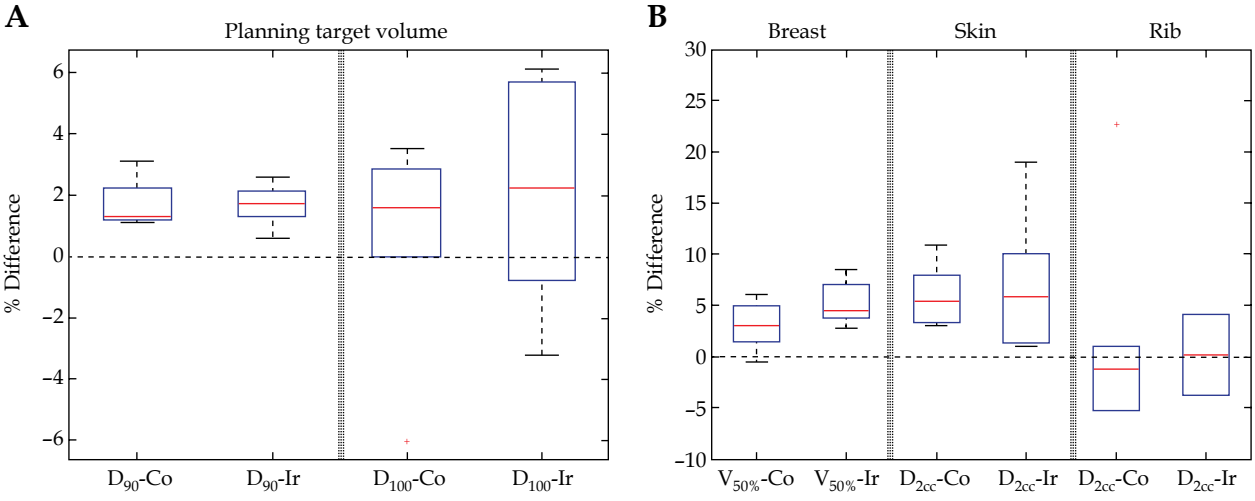

Fig. 5. Comparison of dose-volume histogram (DVH) indices calculated using the TG-43 and Monte Carlo (MC) dose distributions for clinically equivalent ^{60}Co and ^{192}Ir breast treatment plans. Box plots summarize the distribution of difference in the indices ((IndexTG-43-IndexMC)/IndexMC) × 100) with red horizontal lines marking the median, boxes marking the interquartile range, whiskers extending to 1.5 times the interquartile range, and crosses marking outliers

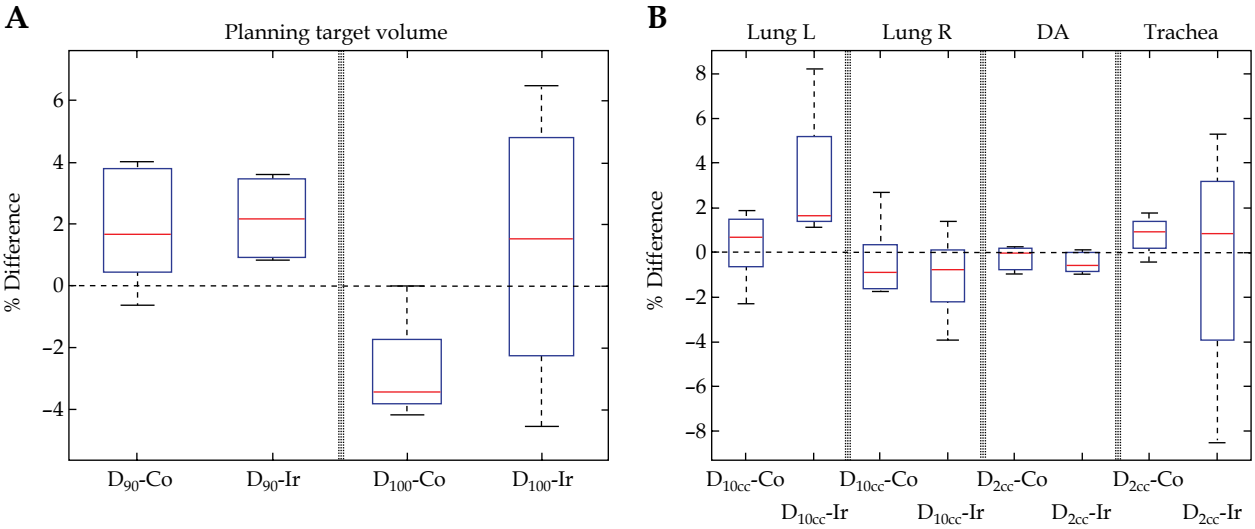

Fig. 6. Same as Figure 5, for ^{60}Co and ^{192}Ir esophageal treatment plans

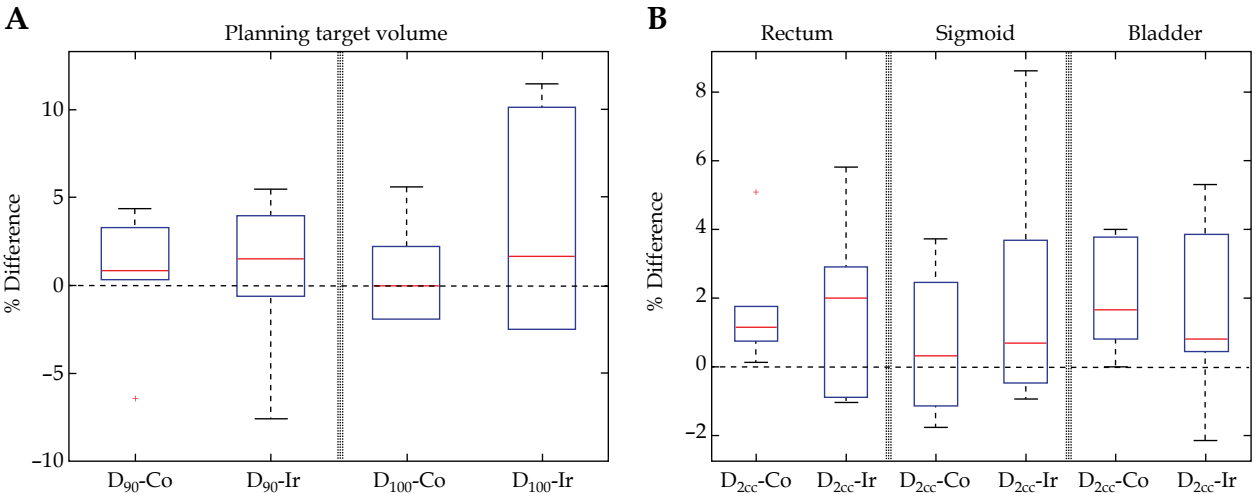

Fig. 7. Same as Figure 5, for ^{60}Co and ^{192}Ir cervical treatment plans

work, although the dose is considerably overestimated by TG-43 for ^{192}Ir (Figure 2), the value of D_{2cc} is determined from the closest source dwell position, leading to comparable median differences for ^{60}Co and ^{192}Ir. Median percentage differences in D_{2cc} between TG-43 and MC results are of the order of 4% and 6% for ^{60}Co and ^{192}Ir, respectively, and a larger dispersion is observed for ^{192}Ir, where difference reaches up to 19%. Regarding the ribs, since $D_{w,m}$ is reported, and hence the expected effect of this high Z – high density material is reduced for ^{192}Ir [36], the altered scattered conditions due to the presence of the lung prevail leading to comparable median percentage differences for ^{192}Ir and ^{60}Co.

Figure 6 summarizes results of the comparison between DVH indices, calculated from the TG-43 and MC dose distributions in equivalent plans for esophageal patients using the ^{60}Co and the ^{192}Ir source. In Figure 6A, median differences for PTV coverage are comparable for ^{60}Co and ^{192}Ir, presenting however a larger dispersion for ^{192}Ir. The median D_{90} is overestimated by TG-43 by about 2% in both ^{60}Co and ^{192}Ir plans, while the minimum dose received by the PTV (D_{100}) is underestimated by ~4% for ^{60}Co and overestimated by ~2% for ^{192}Ir, with the latter however, presenting a wide distribution of differences.

DVH indices for the OARs are summarized in Figure 6B. Regarding the right lung, which is closer to the target, TG-43 deviations are comparable for both treatments showing a median TG-43 underestimation of D_{10cc} on the order of 1%. For the left lung however, TG-43 overestimates D_{10cc} for both treatments with median differences from MC of the order of 1% for ^{60}Co and 2% for ^{192}Ir, and a larger dispersion observed for ^{192}Ir, with differences up to 8%. These results are in accordance with findings presented in Figure 2. Regarding the aorta, differences are within 1% for both treatments. For the aorta, median percentage differences in D_{2cc} are close to 1% for both treatments, with the distribution of differences presenting a considerable dispersion for ^{192}Ir.

Figure 7 summarizes the same comparison of DVH indices for the cervical treatment plans. Median differences in coverage indices for the PTV in Figure 7A are comparable between ^{60}Co and ^{192}Ir treatments, exhibiting a larger dispersion for the latter. In Figure 7B, a general overestimation is observed for all the reported indices. For the rectum, TG-43 overestimates D_{2cc} with median differences of about 1% and 2% for ^{60}Co and ^{192}Ir, respectively, demonstrating a wider dispersion for ^{192}Ir. The same general observations apply for the sigmoid. For the bladder, the median of the difference is greater for ^{60}Co (~2%) than for ^{192}Ir (~0.75%), demonstrating however a wider dispersion again for ^{192}Ir.

Discussion

Besides the introduction of image-based dose calculation algorithms for ^{192}Ir, TG-43 remains the prevalent method for the clinical treatment planning dosimetry in HDR brachytherapy applications. While the equivalence of ^{60}Co and ^{192}Ir brachytherapy has been established in a number of studies in the literature [1,2,3,4,5,6,8,10,11,12], the relative effects of inhomogeneities and patient specific scatter conditions have not been considered. These effects were studied retrospectively in this work, through the comparison of TG-43 based dosimetry with corresponding MC results in groups of clinically equivalent plans with ^{60}Co and ^{192}Ir HDR sources for breast, esophageal, and cervical treatments.

The comparison between TG-43 and MC for breast interstitial ^{192}Ir HDR treatments has been reviewed in the literature and can serve as an indirect validation. In this work, TG-43 was found to overestimate the dose distribution in the whole patient anatomy for ^{192}Ir, apart from the lung, where differences depend on distance from the implant and the patient contour as well as the thickness of lung and/or adipose tissue lying between the points of interest and the implant. This overestimation is position dependent, being small in magnitude (of the order of 2%) in the relatively high-dose region (> 50% of the prescribed dose) and increasing (up to 25%) with distance from the implant and proximity to the external contour. For the lung inhomogeneity, TG-43 presents an overestimation in the organ part close to the target. Along the lung, a large dose underestimation (exceeding 10% in distances far away from the target) is observed, mainly due to the decreased attenuation of the lung inhomogeneity relative to water assumed in TG-43 conditions. Regarding the skin, the TG-43 formalism presents a considerable overestimation (of the order of 5%, reaching up to 25%). The degree of this overestimation depends strongly on the distance of the skin from the target. From a clinical point of view however, this overestimation is on the safe side. Considerable differences (> 5%) between TG-43 and MC calculations observed in structures other than the skin, correspond to lower isodoses (< 50%) thus being of minimal clinical importance, since they lead to minor differences in terms of DVH and plan quality indices clinically used for plan evaluation. Results of this study are in accordance with previous studies investigating the effect of tissue inhomogeneities and patient specific scatter conditions in ^{192}Ir HDR breast brachytherapy [32,37,38,39]. Zourari *et al*. [38,39] used CT-based patient geometries to compare TG-43 with MBDCAs incorporated in two commercially available TPSs for ^{192}Ir HDR brachytherapy, and reported similar differences with that observed in this study using MC simulations. Pantelis *et al*. [37] reported that TG-43 overestimates lung and skin dose by 5-10%, using a patient-equivalent mathematical phantom. Peppa *et al*. [32] compared $D_{m,m}$ determined from MC simulations to $D_{w,m}$ from TG-43-based dose calculations in patient CT-based geometries, and reported a TG-43 dose overestimation for target, skin, and lung, compatible with corresponding results of this work.

Regarding the comparison between TG-43 and MC in this work for ^{60}Co and ^{192}Ir plans, for breast, the mean dose to the lung as well as dose to the healthy breast tissue were considerably overestimated by TG-43 in ^{192}Ir treatments. For the skin, although dose was considerably overestimated by TG-43 for ^{192}Ir, the indices were determined from the closest source dwell position leading to comparable differences between ^{60}Co and ^{192}Ir. For the ribs, since MC results of this work correspond to $D_{w,m}$, comparable medi-

an percentage differences were observed for ^{192}Ir and ^{60}Co due to the alteration of scatter conditions by the presence of the lung. Similar differences were observed for esophageal treatments, which are attributed to the effect of density inhomogeneities around the catheter. For the right lung, which is typically closer to the target, so that the primary radiation dose component prevails, TG-43 differences were comparable for ^{60}Co and ^{192}Ir. As distance from the implant increased, e.g., for the left lung, and the scatter contribution becomes more important for ^{192}Ir, percentage dose differences also increased. As for the gynecological cases, a general dose overestimation was observed by TG-43, which had a greater effect on the OARs for ^{192}Ir.

The differences observed between TG-43 and MC dose results between ^{60}Co and ^{192}Ir plans can be explained by considering the difference in the relative importance of primary and scatter dose for the two radionuclides [3,40]. At points inside or close to the treated targets, an agreement within 2% was observed between TG43 and corresponding MC dose results in all the studied cases, which is attributed to the relatively increased contribution of primary photons to dose at these points for both ^{192}Ir and ^{60}Co treatment plans. As distance from source dwell positions increases, the relative contribution of scattered photons to dose increases. This increase is more pronounced for ^{192}Ir compared to ^{60}Co photon energies at the presented distances [3,40]. This explains the greatest TG43 overestimation for ^{192}Ir in the OARs (healthy breast tissue, heart, and spinal cord in the esophageal cases, bladder, sigmoid, and rectum in the gynecological cases). For the lungs, a comparable TG43 dose underestimation was observed for ^{192}Ir and ^{60}Co, which is attributed to the increased contribution of the primary dose component in the low density lung tissue relative to water, assumed by the TG43 dose calculation algorithm. As distance from the source dwell positions increases, the scatter contribution becomes more important, and the corresponding percentage dose differences for points inside the lungs are larger for ^{192}Ir relative to ^{60}Co. The relative importance of the scatter dose component becomes predominant at greater distance from a source for the ^{60}Co energies [3] (distances greater than one mean free path of about 12 cm in water). The increased relative importance of scatter radiation to dose for ^{192}Ir relative to ^{60}Co also explains the higher variation of clinically used indices in the studied treatment plans for ^{192}Ir.

Most of the above mentioned differences however, apply to the relatively low dose region, and in spite of high local values (> 5%), they correspond to less than 20% of the prescribed dose. These differences are therefore of reduced clinical importance. Still, in case of patient re-irradiation and/or evaluation of combined treatments (e.g., brachytherapy boost following whole breast external beam radiation therapy), accurate dosimetry to the skin and other critical organs could be valuable for long-term toxicity determination. Improved dosimetry in the low dose region might also be valuable for the assessment of secondary cancer induction risk.

Limitations associated with the design and the implementation of this work include the size of the samples of treatment cases studied, the approximation of dose by collisional kerma in patient-specific simulations of this work for ^{60}Co to promote efficiency, potential volume averaging effects in MC results due to the resolution in the patient CT imaging series, and the fact that dosimetry results corresponding to voxels within or partially including; the applicators were not excluded. Nevertheless, the generality of findings is not flawed since the high-dose volume close to the sources was discarded from the comparison between TG-43 and MC results, and findings of this comparison for ^{192}Ir are in accordance with previous results in the literature.

Conclusions

The effects of inhomogeneities and patient specific scatter conditions were studied retrospectively, through the comparison of TG-43 based dosimetry with corresponding Monte Carlo results in groups of clinically equivalent plans with ^{60}Co and ^{192}Ir HDR sources for breast, esophageal, and cervical treatments. The comparison between TG-43 and MC for ^{60}Co and ^{192}Ir plans showed a TG-43 dose overestimation in the whole patient anatomy, apart from the lungs where dose differences present a reversed sign depending on depth within the organ, with a greater magnitude for ^{192}Ir treatments. For the target, subtle differences (of the order of 2%) were observed in the evaluated DVH indices in all three patient groups for both ^{60}Co and ^{192}Ir, with a greater dispersion however for ^{192}Ir. For the OARs, errors induced by the TG-43 assumptions were smaller in magnitude and/or range for ^{60}Co relative to ^{192}Ir treatments, with a greater dispersion within the patient groups for the latter. Owing to the higher energy of photon emissions, ^{60}Co HDR sources are more amenable to the TG-43 assumptions in clinical treatment planning dosimetry.

Acknowledgement

K. Zourari was financially supported by Eckert & Ziegler BEBIG GmbH. The authors gratefully acknowledge Michael Andrássy, Senior Physicist at Eckert & Ziegler BEBIG GmbH, for useful discussions and information on source geometries.

Disclosure

Authors report no conflict of interest.

References

1. Ntekim A, Adenipekun A, Akinlade B et al. High Dose Rate Brachytherapy in the Treatment of cervical cancer: preliminary experience with cobalt 60 Radionuclide source-A Prospective Study. *Clin Med Insights Oncol* 2010; 4: 89-94.
2. Mosalaei A, Mohammadianpanah M, Omidvari S et al. High-dose rate brachytherapy in the treatment of carcinoma of uterine cervix: twenty-year experience with cobalt after-loading system. *Int J Gynecol Cancer* 2006; 16: 1101-1105.
3. Strohmaier S, Zwierzchowski G. Comparison of 60Co and 192Ir sources in HDR brachytherapy. *J Contemp Brachytherapy* 2011; 3: 199-208.
4. Richter J, Baier K, Flentje M. Comparison of 60cobalt and 192iridium sources in high dose rate afterloading brachytherapy. *Strahlenther Onkol* 2008; 184: 187-192.

5. Park D, Kim YS, Park SH et al. A comparison of dose distributions of HDR intracavitary brachytherapy using different sources and treatment planning systems. *Appl Radiat Isot* 2009; 67: 1426-1431.
6. Palmer A, Hayman O, Muscat S. Treatment planning study of the 3D dosimetric differences between Co-60 and Ir-192 sources in high dose rate (HDR) brachytherapy for cervix cancer. *J Contemp Brachytherapy* 2012; 1: 52-59.
7. Safigholi H, Han DY, Mashouf S et al. Direction Modulated Brachytherapy (DMBT) for Treatment of Cervical Cancer: A Planning Study with 192Ir, 60Co, and 169Yb HDR Sources. *Med Phys* 2017; 44: 6538-6547.
8. Candela-Juan C, Perez-Calatayud J, Rivard MJ. Calculated organ doses using Monte Carlo simulations in a reference male phantom undergoing HDR brachytherapy applied to localized prostate. *Med Phys* 2013; 40: 033901.
9. Safigholi H, Meigooni AS, Song WY. Comparison of 192 Ir, 169 Yb, and 60 Co high-dose rate brachytherapy sources for skin cancer treatment. *Med Phys* 2017; 44: 4426-4436.
10. Baltas D, Lymperopoulou G, Zamboglou N. On the use of HDR 60Co source with the MammoSite radiation therapy system. *Med Phys* 2008; 35: 5263-5268.
11. Zehtabian M, Sina S, Rivard MJ et al. Evaluation of BEBIG HDR 60Co system for non-invasive image-guided breast brachytherapy. *J Contemp Brachytherapy* 2015; 7: 469-478.
12. Sinnatamby M, Nagarajan V, Kanipakam Sathyanarayana R et al. Study of the dosimetric differences between 192Ir and 60Co sources of high dose rate brachytherapy for breast interstitial implant. *Reports Pract Oncol Radiother* 2016; 21: 453-459.
13. Papagiannis P, Pantelis E, Karaiskos P. Current state of the art brachytherapy treatment planning dosimetry algorithms. *Br J Radiol* 2014; 87: 20140163.
14. Sloboda RS, Morrison H, Cawston-Grant B et al. A brief look at model-based dose calculation principles, practicalities, and promise. *J Contemp Brachytherapy* 2017; 9: 79-88.
15. Nath R, Anderson LL, Luxton G et al. Dosimetry of interstitial brachytherapy sources: recommendations of the AAPM Radiation Therapy Committee Task Group No. 43. American Association of Physicists in Medicine. *Med Phys* 1995; 22: 209-234.
16. Granero D, Pérez-Calatayud J, Ballester F. Technical note: Dosimetric study of a new Co-60 source used in brachytherapy. *Med Phys* 2007; 34: 3485.
17. Granero D, Pérez-Calatayud J, Ballester F. Monte Carlo study of the dose rate distributions for the Ir2.A85-2 and Ir2.A85-1 Ir-192 afterloading sources. *Med Phys* 2008; 35: 1280-1287.
18. Eckert & Ziegler BEBIG. HDR Applicators & Accessories.
19. Chassagne D, Dutreix A, Almond P et al. Report 38. *J Int Comm Radiat Units Meas* 1985; os20:NP-NP.
20. Berger D, Kauer-Dorner D, Seitz W et al. Concepts for critical organ dosimetry in three-dimensional image-based breast brachytherapy. *Brachytherapy* 2008; 7: 320-326.
21. Pelowitz DB, Goorley JT, James MR et al. MCNP6 user's manual, 2013.
22. Cullen DE, Hubbell JH, Kissel L. EPDL97: The evaluated photon data library '97', UCRL-LR-50400 Vol 6 Rev 5. Springfield, VA: 1997.
23. Pantelis E, Peppa V, Lahanas V et al. BrachyGuide: A brachytherapy-dedicated DICOM RT viewer and interface to Monte Carlo simulation software. *J Appl Clin Med Phys* 2015; 16: 208-218.
24. National Nuclear Data Center, information extracted from the NuDat 2 database; http://www.nndc.bnl.gov/nudat2/
25. Goorley T, James M, Booth T et al. Initial MCNP6 Release Overview. *Nucl Technol* 2012; 180: 298-315.
26. Hubbell JH, Seltzer SM. Tables of X-Ray Mass Attenuation Coefficients and Mass Energy-Absorption Coefficients (version 1.4). Natl Inst Stand Technol Gaithersburg, 1995.
27. Papagiannis P, Angelopoulos A, Pantelis E et al. Monte Carlo dosimetry of [sup 60]Co HDR brachytherapy sources. *Med Phys* 2003; 30: 712-721.
28. Ballester F, Granero D, Pérez-Calatayud J et al. Evaluation of high-energy brachytherapy source electronic disequilibrium and dose from emitted electrons. *Med Phys* 2009; 36: 4250-4256.
29. Schneider W, Bortfeld T, Schlegel W et al. Correlation between CT numbers and tissue parameters needed for Monte Carlo simulations of clinical dose distributions. *Phys Med Biol* 2000; 45: 459-478.
30. Peppa V, Pappas E, Major T et al. On the impact of improved dosimetric accuracy on head and neck high dose rate brachytherapy. *Radiother Oncol* 2016; 120: 92-97.
31. Peppa V, Pantelis E, Pappas E et al. A user-oriented procedure for the commissioning and quality assurance testing of treatment planning system dosimetry in high-dose-rate brachytherapy. *Brachytherapy* 2016; 15: 252-262.
32. Peppa V, Pappas EP, Karaiskos P et al. Dosimetric and radiobiological comparison of TG-43 and Monte Carlo calculations in 192Ir breast brachytherapy applications. *Phys Med* 2016; 32: 1245-1251.
33. Peppa V, Zourari K, Pantelis E et al. Tissue segmentation significance for individualized 192Ir brachytherapy dosimetry. *Radiother Oncol* 2013; 106: S371.
34. Ballester F, Carlsson Tedgren Å, Granero D et al. A generic high-dose rate 192Ir brachytherapy source for evaluation of model-based dose calculations beyond the TG-43 formalism. *Med Phys* 2015; 42: 3048-3062.
35. Perez-Calatayud J, Ballester F, Das RK et al. Dose calculation for photon-emitting brachytherapy sources with average energy higher than 50 keV: Report of the AAPM and ESTRO. *Med Phys* 2012; 39: 2904-2929.
36. Fonseca GP, Tedgren ÅC, Reniers B et al. Dose specification for ^{192}Ir high dose rate brachytherapy in terms of dose-to-water-in-medium and dose-to-medium-in-medium. *Phys Med Biol* 2015; 60: 4565-4579.
37. Pantelis E, Papagiannis P, Karaiskos P et al. The effect of finite patient dimensions and tissue inhomogeneities on dosimetry planning of 192Ir HDR breast brachytherapy: a Monte Carlo dose verification study. *Int J Radiat Oncol Biol Phys* 2005; 61: 1596-1602.
38. Zourari K, Major T, Herein A et al. A retrospective dosimetric comparison of TG43 and a commercially available MBDCA for an APBI brachytherapy patient cohort. *Phys Medica* 2015; 31: 669-676.
39. Zourari K, Pantelis E, Moutsatsos A et al. Dosimetric accuracy of a deterministic radiation transport based (192)Ir brachytherapy treatment planning system. Part III. Comparison to Monte Carlo simulation in voxelized anatomical computational models. *Med Phys* 2013; 40: 11712.
40. Sakelliou L, Sakellariou K, Sarigiannis K et al. Dose rate distributions around Co-60, Cs-137, Au-198, Ir-192, Am-241, I-125 (models 6702 and 6711) brachytherapy sources and nuclide Tc-99m. *Phys Med Biol* 1992; 37: 1859-1872.